Effect of Water on the Changes in Morphology and Proton Conductivity for the Highly Crystalline Hydrocarbon Polymer Electrolyte Membrane for Fuel Cells

Mohammad A. Barique,* Libin Wu,† Naohiko Takimoto, Koh Kidena, and Akihiro Ohira*

Polymer Electrolyte Fuel Cell Cutting-edge Research Center (FC-Cubic), National Institute of Advanced Industrial Science and Technology (AIST), 2-3-26 Aomi, Koto-ku, Tokyo 135-0064, Japan

Received: June 5, 2009; Revised Manuscript Received: September 24, 2009

The effects of water on the changes in morphology of sulfonated poly(phenylene sulfide) (SPPS) hydrocarbon polymer electrolyte membranes (PEM) with an ion exchange capacity (IEC) of 0−2.0 mequiv/g are investigated using small-angle X-ray scattering (SAXS) and atomic force microscopy (AFM). Wide-angle X-ray scattering (WAXS) was used to characterize the effect of direct sulfonation on the changes in membrane crystalline structure, and it was found that the crystallinity and crystallite domain size decrease and the volume of the amorphous region in the SPPS membranes increases with increasing IEC. The experimental data have been fitted to the Porod law for approaching the analysis of the sharpness of the polymer/water interface, development of the proton channel, or dispersion of water in the hydrated membranes. Porod plots showed positive deviation which revealed that the polymer/water interface in the hydrated SPPS membrane is not smooth but diffused and a well-developed proton channel does not form in the membrane.

1. Introduction

The polymer electrolyte membrane (PEM) is a key component of the polymer electrolyte fuel cell (PEFC) for transferring protons from the anode to the cathode. Although well-known perfluorinated ionomer Nafion membranes show superior performance in PEFCs operating at moderate temperatures (<90 °C) and high relative humidity with pure hydrogen as a fuel, but their inherently high cost of production, low conductivity at low humidity or high temperature have limited their usages.[1] Thus, development of new materials is essential in order to overcome these critical problems. The hydrocarbon (HC) type materials have recently received great attention as one of the most important and popular materials for PEFC membrane. A promising route to high-performance PEM is the use of hydrocarbon polymers.[2] The advantages of HC-type ionomers are that they are cheaper than the perfluorinated ionomers currently used and have better mechanical properties and thermal stability which can lead to a suitable design.[3,4] Some superior HC-type membranes have been developed, and it has been reported that those membranes possess high water absorption capacity and proton conductivities at high temperatures and low humidity, with sufficient thermal and mechanical stabilities.[5,6] Direct sulfonation of well-established engineering plastic-based HC-type polymers, in particular, poly(ether ether ketone) (PEEK),[1,7−9] poly(ether sulfone) (PES),[10−14] poly(*p*-phenylene) (PP),[15−18] and so on is one of the most effective methods for the production of PEM for advanced technologies such as electrodialysis and PEFCs.[19] However, for practical use of PEFC and for further improvements to secure the high proton conduction at lower humidity and at high-temperature operation, high chemical and mechanical durabilities are essential. To solve these problems, we need to characterize and control the membrane morphology related not only to mass transportation of protons, water, and gases but also the dimensional stability related to chemical and mechanical properties. Though there are some reports which discussed the influence of a particular ion exchange capacity (IEC) on the physical properties of PEM, the effects of varied IEC on the morphology of membranes have not been discussed sufficiently.

SCHEME 1: Schematic Diagram of Sulfonated Poly(1,4-phenylene sulfide)

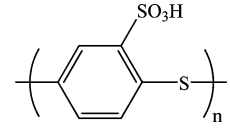

We have carried out a systematic study of the morphology of a series of PPS membranes with lower to higher IEC (0−2.0 mequiv/g). Our present highly crystalline starting PPS (IEC:0) sample is a high-performance semicrystalline wholly aromatic polymer with outstanding high-temperature stability, good chemical and flame resistances, excellent electrical insulation, antiaging, and precision moldability.[20,21] Furthermore, sulfonated PPS (SPPS) membranes that we report here can disregard the effect of morphological change originated from the process of membrane formation because the sulfonation reaction is performed directly from the membrane which is prepared by melt extrusion of highly crystalline PPS. The present way, i.e., the direct sulfonation of membrane, gives us an opportunity to investigate the effect of IEC on morphological features, to consider the formation of an interface between hydrophobic and hydrophilic domains, and to study the hydration behavior without any complicated factors regarding morphology and IEC. A schematic diagram of SPPS is shown in Scheme 1.[22] Schuster et al. prepared poly(phenylene sulfide sulfone) ($sPSO_2$) with high IEC (4.5 mequiv/g) by oxidizing the poly(phenylene sulfide sulfone) (sPSS) and found that at higher temperature (110−160 °C) and low relative humidities (50−15% RH) the proton conductivity exceeds that of Nafion by a factor of 5−7, but the $sPSO_2$ is water-soluble and brittle in the dry state.[23]

* Corresponding authors. Phone: +81 3 3599 8550. Fax: +81 3 3599 8554. E-mail: ma.barique@aist.go.jp (M.A.B.); a-oohira@aist.go.jp (A.O.).

† Present address: Dept. Organic and Polymeric Materials, Tokyo Institute of Technology, Ookayama 2-12-1-S5-20, Meguro-ku, Tokyo, 152-8552, Japan. Phone: +81-3-5734-2581. Fax: +81-3-5734-2581.

10.1021/jp905297m CCC: $40.75
Published on Web 11/12/2009

In this paper, we report the effect of direct sulfonation on the changes in morphology of highly crystalline starting PPS hydrocarbon membranes and the effect of water on the changes in sharpness of the polymer/water interface, development of proton channel, and proton conduction in the SPPS electrolyte membranes for PEFCs.

2. Experimental Methods

Sulfonation of PPS Membranes. The sulfonation of commercial PPS membranes (thickness 50 μm) was performed by the following procedure.[24] A 50 g portion of dichloromethane and 0.117 g of chlorosulfonic acid were weighed and put in a 50 mL glass flask to prepare a chlorosulfonic acid solution. A 0.117 g portion of PPS membrane was weighed, immersed in the chlorosulfonic acid solution, and left for 20 h at room temperature. Then, the sulfonated PPS membrane was recovered from the solution and rinsed with ion-exchanged water until it became neutral. The SPPS membrane was again immersed in 50 mL of ion-exchanged water and left for 20 h at room temperature. The membrane was recovered and dried under reduced pressure at 80 °C for 3 h. The IEC value of the membrane was then determined by back-titration. Other higher IEC value membranes were prepared in the same procedure by gradual increase of the amount of chlorosulfonic acid. To prepare every IEC value film, the amount of chlorosulfonic acid was adjusted on the basis of the aromatic unit of poly(phenylene sulfide).

Titration Procedure. The IEC of the SPPS membranes was determined through the back-titration method. PPS membranes in acid (H^+) form were dried overnight at 100 °C under vacuum, weighed, and then immersed in saturated NaCl for 24 h. The amount of H^+ ion released from the membrane samples was determined by titration with 0.01 M NaOH using phenolphthalein as an indicator. IEC was calculated by the following equation:

$$\mathrm{IEC} = \frac{C \times V}{M} \tag{1}$$

where C and V are the concentration and volume of NaOH, respectively, and M is the weight of the membrane.

Wide-Angle X-ray (WAXS) Measurements. WAXS measurements were made for the membranes with varied IEC using a Rigaku Ultima-IV X-ray diffractometer with Ni-filtered Cu Kα radiation ($\lambda = 0.15418$ nm) operated at 40 kV and 40 mA in air, in the symmetrical reflection mode. Samples were scanned under diffraction angle in the 2θ range of 5−90° with a step scan interval of 0.2°/min. The profiles were smoothed, and the background (dark scattering) was subtracted from all of the data.

Small-Angle X-ray Scattering (SAXS) Measurements. Two-dimensional, point-collimated SAXS measurements were performed using a Rigaku NANO-Viewer with Ni-filtered Cu Kα radiation ($\lambda = 0.15418$ nm), which was finely focused by a confocal max-flux mirror (CMF) and collimated into the Rigaku-made airtight sample chamber with Kapton windows using a three-slit system. The chamber was then connected with a humidity generator (model HUM-1) under ambient conditions of temperature and relative humidity (RH). SAXS was operated at 40 kV and 30 mA power beam. X-ray scattering patterns were recorded for 6 h at 40 °C for every constant relative humidity (RH). The experiments were carried out in the transmission mode. Two-dimensional SAXS patterns were recorded on a sheet of an imaging plate (IP), and the sample-to-IP distance was set to 60 cm. The signals from the air and dark scattering were subtracted from every SAXS image pattern, and then, the two-dimensional SAXS pattern was integrated by Rigaku software, to obtain the scattering pattern as a function of $q = (4\pi \sin\theta)/\lambda$, where q is the phonon vector, 2θ the scattering angle, and λ the X-ray wavelength.

Water Uptake and Proton Conductivity Measurements. Water uptake and proton conductivity were measured using an isothermal absorption measurement system (MSB-AD-V-FC, BEL Japan Inc.) equipped with an impedance analyzer (Solartron SI 1260). The system enabled the simultaneous measurements of water uptake and proton conductivity in the same chamber. Each membrane sample was dried at 80 °C for 1 h under dry nitrogen flow and then exposed to a humidified nitrogen environment at 80 °C. After the weight of each sample reached equilibrium, the sample weight and proton conductivity were determined sequentially. Humidity conditions were changed stepwise from 10% RH to 95% RH. The water uptake of membranes was calculated as the water volume fraction on the basis of the dry weight and volume of the samples using water volume fraction:

$$V_{\mathrm{f,H_2O}} = \frac{(W_{\mathrm{wet}} - W_{\mathrm{dry}})/d_{\mathrm{H_2O}}}{V_{\mathrm{dry}}} \tag{2}$$

where W_{wet} and W_{dry} are the weights of the wet and dry membranes, respectively, and V_{dry} is the volume of the dry membranes. The water density $d_{\mathrm{H_2O}}$ was 1 g/cm^3.[25]

Proton conductivity was measured using a four-point probe cell. The AC impedance spectrum was recorded from 10 Hz to 100 kHz using an impedance analyzer. Proton conductivity was calculated from dry membrane thickness, and membrane resistance was chosen at the frequency that produced the minimum imaginary response.

Number of Water Molecules per Sulfonated Group. The number of water molecules per sulfonated group at each relative humidity, $\lambda(\mathrm{H_2O/SO_3H})$, was calculated using the IEC value of SPPS membranes with the following equation:

$$\lambda = \frac{\text{water uptake (\%)} \times 10}{\mathrm{IEC} \times \mathrm{MW_{H_2O}}} \tag{3}$$

where $\mathrm{MW_{H_2O}}$ is the molecular weight of water (18.01 g mol^{-1}).

3. Results and Discussion

Effect of Sulfonation Level on the Changes in Crystalline Morphology of SPPS Membranes. WAXS was performed to investigate the morphology of nonsulfonated (IEC:0) and sulfonated PPS membranes with varied IEC, as shown in Figure 1. The nonsulfonated PPS membrane showed an intense and very sharp peak at around $2\theta = 20.4°$ which results from a convolution of lamellar crystals and amorphous scattering.[26] The peak arises from the (110) plane of orthorhombic PPS structure.[27,28]

The peak intensity gradually decreases and broadens with increasing IEC level which indicates the gradual decrease of the lamellar crystallite domain size. The peak maxima moves slightly to a lower angle from IEC level 1.6, indicating that in higher IEC membranes the smaller crystallite domains were distantly spaced with higher free volume compared with lower IEC membranes. WAXS profiles also indicated that although the membranes lost their crystalline structure after a sufficient

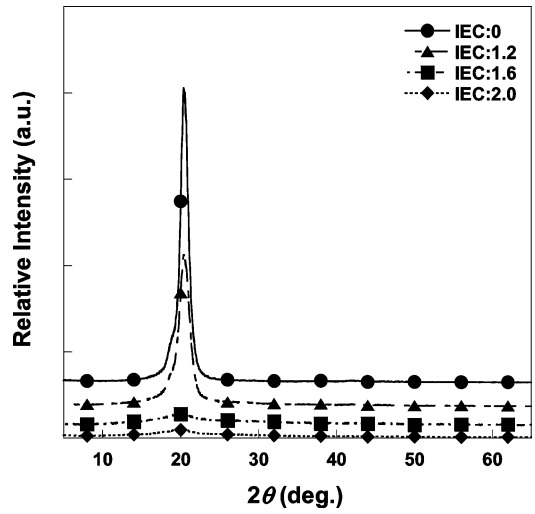

Figure 1. WAXS profiles for SPPS membranes with varied IEC.

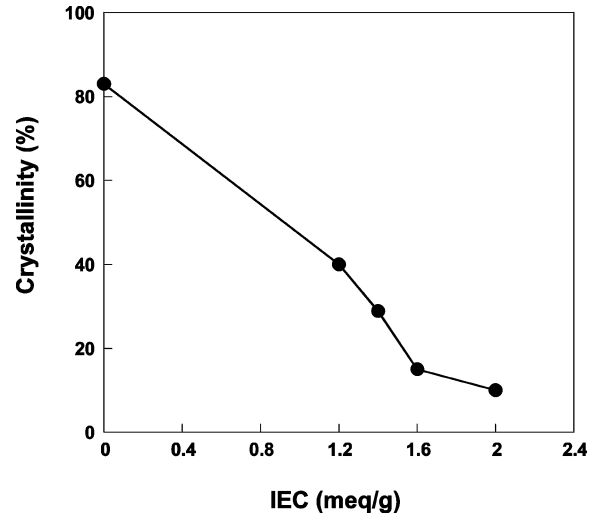

Figure 2. Effect of IEC on the crystallinity of SPPS membranes. Highly crystalline starting PPS film was directly sulfonated.

degree of sulfonation a very small amount of crystallinity was retained up to IEC level 2.0. From the peak position and width, the crystallite domain size D_{hkl} was calculated using the Scherrer equation

$$D_{hkl} = \frac{\lambda}{\beta_{hkl} \cos \theta_{hkl}} \tag{4}$$

where λ is the X-ray wavelength, β_{hkl} is the full width at half-maximum (fwhm) of the profiles (after correction for apparatus broadening), and θ is the Bragg angle of *hkl* reflection. It was found that the crystallite domain size decreases with increasing IEC. The degree of crystallinity for varied IEC membranes was calculated from their WAXS profiles using the following equation:

$$\chi_c = 1 - \frac{I_a}{(I_a + I_c)} \tag{5}$$

where I_c is the integrated intensity of the crystalline volume and I_a is the integrated intensity of the amorphous volume fraction of the sample. The crystallinity of sulfonated membranes decreased with increasing IEC and is shown in Figure 2.

For every IEC membrane, sulfonation starts from the surface and decreases the membrane crystallinity. Up to IEC level 1.6, crystallinity decreases very steeply, but from IEC 1.6 to 2.0, crystallinity does not change so remarkably, which is shown in Figure 2. We consider the PPS crystallite domains in the membrane as a core−shell model; due to the sulfonation reaction, the sulfonic acid group ($-SO_3H$) initially starts to attach to the phenylene rings of the amorphous region (the shell) of the system. With increasing concentration of chlorosulfonic acid, the sulfonation reaction proceeds to more depth from the surface of the membrane with rupturing the crystallite domains (the core) which results in a greater decrease in the crystallite core size with increasing IEC. The sulfonation reaction proceeds into the inner chains of the crystallite domains and changes them into amorphous, and thus, the volume of the amorphous region increases. A schematic diagram of the sulfonation reaction in PPS membrane is illustrated in Scheme 2. The effect of IEC on the crystallite size and interdomain spacings of the membranes is shown in Table 1.

The crystallite domain size decreases with increasing IEC, but the interdomain spacings for the (110) plane do not change remarkably.[28] As can be seen from Figure 1, a very broad peak still retained up to IEC:2.0 (highest IEC of the present work) membrane, which indicated that though the membrane lost its three-dimensional crystalline structure after a sufficient sulfonation a small amount of tightly packed crystalline seeds are still retained in the membrane. We consider that up to IEC:1.6 crystallinity decreases smoothly, but after that with higher concentrated chlorosulfonic acid though sulfonation proceeds but not smoothly because the sulfonation reaction approaches the crystalline seeds in the depth of the membrane which is comparatively hard to be sulfonated, so the crystallinity does not decrease remarkably. Swier et al. also found that sulfonation of poly(ether ketone ketone) (PEKK) ionomers decreased its crystallinity, which was shown by the loss of the crystalline reflections in the wide-angle X-ray diffraction.[29] Min et al. observed that increased sulfonation level causes reduction of crystallite size and their uniform distribution throughout the sulfonated bisphenol A polyetherimide (SPEI) matrix.[30] The introduction of pendant $-SO_3H$ groups into the polymer alters chain conformation and packing, increases molecular bulkiness, and accordingly causes the loss of the crystalline domains.[31] Liu et al. worked on the sulfonation of Cardo polyetherketone (PEK-C) and found that the more sulfonic acid groups were introduced, the more amorphous regions formed in the sulfonated PEK-C (SPEK-C) membranes. They also showed that the introduced sulfonic acid groups disturbed the arrangement of PEK-C chains, leading to the crystallinity decreasing in the SPEK-C membranes.[32]

Humidity-Dependent Morphology for Varied IEC Membranes. Generally, the hydrophobic backbone domain and the hydrophilic nanophase containing sulfonic acid groups separate into two phases in the presence of water in the polymer electrolyte membranes. The hydrophobic domain provides the polymers with morphological stability, and the hydrophilic domain is responsible for aggregation of water molecules and transporting protons. SAXS was performed to investigate the changes in morphological properties, such as water dispersion in swelled polymer matrix, development of ionic domains, and

SCHEME 2: Schematic Diagram of Sulfonation Reaction in PPS Membrane

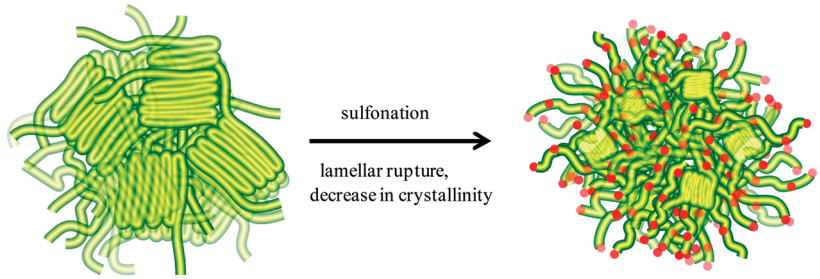

TABLE 1: Effect of IEC on Crystallite Size and Interdomain Spacing in SPPS Membranes

IEC (mequiv/g)	crystallite domain size (nm)	interdomain spacing (nm)
0	12	0.4354
1.2	5	0.4354
1.6	2	0.4440
2.0	1	0.4440

sharpness of polymer/water interface in the SPPS membranes in hydrated states.

The effects of relative humidity on the SAXS integrated intensity for SPPS membranes with varied IEC at 40 °C are shown in Figure 3. A shoulder peak at around $q = 0.5$ nm^{-1} was found for all varied IEC (0−2.0) membranes of the present investigation, which was caused from the electron density contrast between the lamellar crystalline domains and amorphous domains in PPS membranes.[33] In all of the SAXS experiments, the crystalline shoulder peak position almost did not change with increasing relative humidity and was independent of polymer swelling for every IEC samples. From Figure 3a, it was found that the crystalline shoulder peak intensity increases with increasing relative humidity for the IEC:0 membrane. On the other hand, for the sulfonated membrane of IEC:2.0 (Figure 3b), the peak intensity first gradually starts to increase with increasing relative humidity, becomes maximum at around 50% RH, and after that gradually starts to decrease. Finally, at 80% RH, the shoulder peak intensity dropped even to a value of less than 30% RH intensity.

Nonsulfonated PPS membrane has a higher electron density difference between the lamellar crystalline and amorphous phase, and it is reasonable that it shows remarkable increasing intensity with increasing relative humidity. We measured the water uptake of PPS (IEC:0) at 40 °C and found that the membrane is not so hydrophobic and absorbs some water. However, for the sulfonated PPS membranes of every IEC, the amorphous region is sulfonated and as the sulfonic acid groups have affinity to absorb water, so with increasing water the electron density in the water-rich amorphous domain gradually increases. In Figure 3b, a SAXS shoulder peak arises from the electron density contrast between the water-absorbed amorphous and crystal domain of the IEC:2.0 membrane. From the experimental results, we suggest that as the water affinity of the sulfonic acid group (SO_3H) is very high the amorphous domains absorb water rapidly at relatively lower humidity and make ion−water aggregates of different sizes. At around 50% RH, the aggregates become remarkable in size and the electron density of the amorphous domains becomes highest, and that is why the shoulder peak intensity at this RH% region becomes maximum. After that, though, water increases in the membrane but the aggregates do not become larger. On the basis of SAXS profiles for IEC:2.0 in Figure 3b, the effect of the number of water molecules, $\lambda(n\mathrm{H_2O/SO_3H})$, on the SAXS integrated intensity value of the shoulder peak is plotted in Figure 4. As can be seen from the figure, at $\lambda = 3.5$ (corresponds to 50% RH), the peak intensity has the maximum value and the reason for this is discussed above.

A three-dimensional schematic diagram of the effect of relative humidity on the states of water molecules in the SPPS membrane under hydrated conditions is illustrated in Scheme 3. It is shown that the number of water molecules gradually increases with increasing relative humidity, makes ion−water

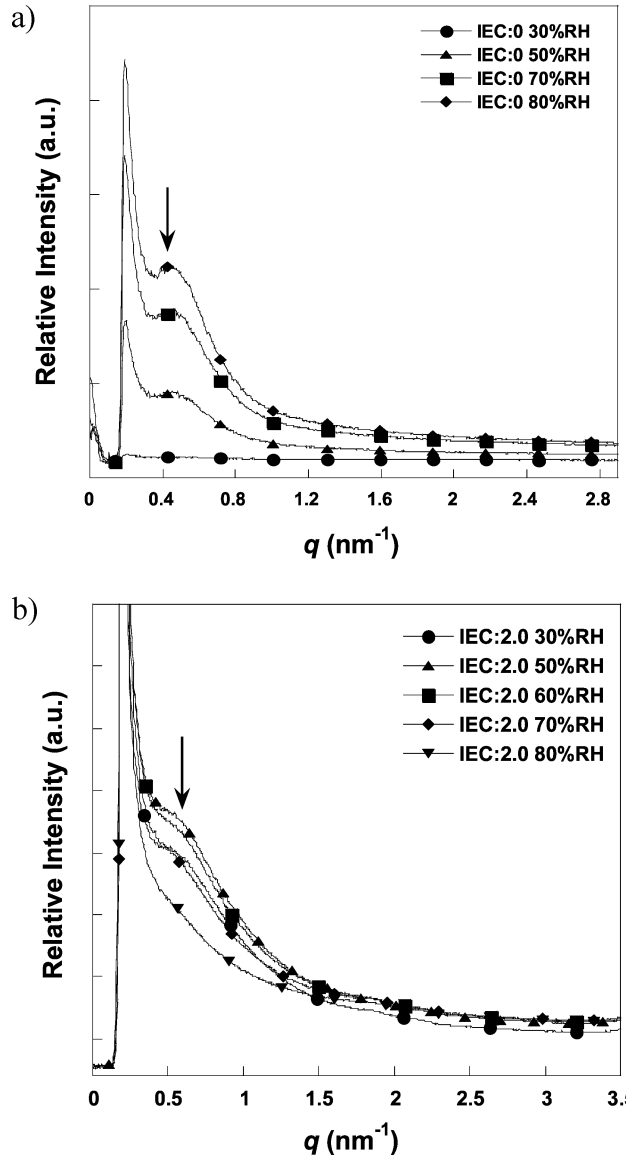

Figure 3. Effect of relative humidity on SAXS scattering for SPPS membranes with (a) IEC:0 and (b) IEC:2.0. The incident X-ray beam was normal to the film surface.

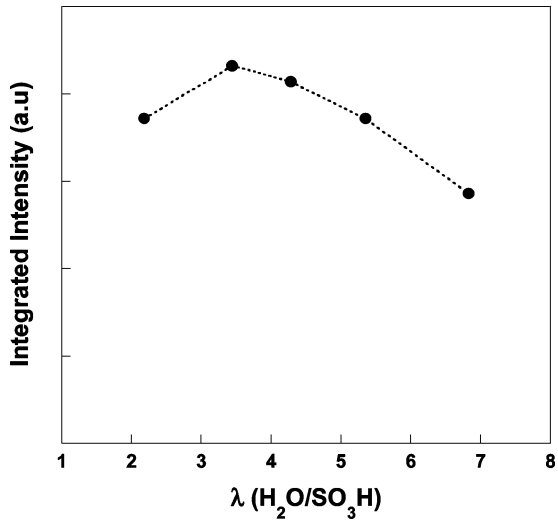

Figure 4. Effect of the number of water molecules, $\lambda(H_2O/SO_3H)$, on the integrated intensity value of the shoulder peak for the IEC:2.0 membrane.

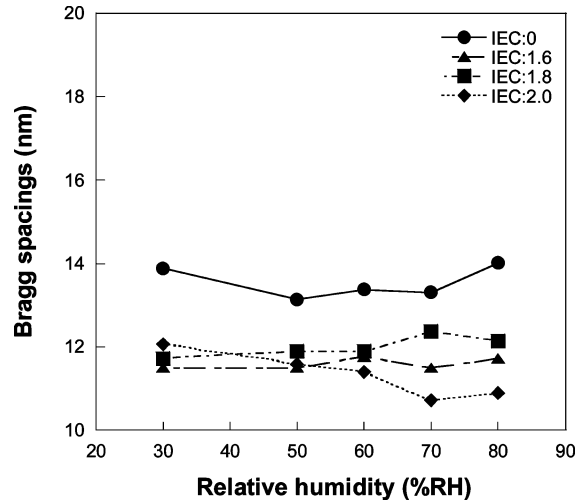

Figure 5. Effect of relative humidity on the Bragg spacings for the shoulder peak at lower scattering angle of SPPS membranes with varied IEC.

aggregates, the aggregate size becomes gradually larger and after that at higher RH% though the number of water molecules increases but those waters do not make the water aggregate more larger rather gradually disperse in the whole membrane. The possible reason for the SAXS shoulder peak intensity fluctuation of the IEC:2.0 membrane may be the PPS backbone chains are very rigid, so there is no scope of intramolecular or even intermolecular mobility and aggregates cannot come closer to increase the number of water molecules in the amorphous domain. In this situation, water−water hydrogen bond interaction becomes stronger than ionic−water affinity and as a result water molecules start to attract each other, arrange themselves, and start to disperse in the membrane. The comparatively larger ion−water aggregates formed at the stage of 50% RH even start to become disperse and smaller in size, and the electron density of the water-rich amorphous domain becomes gradually less with more and more water absorption. Lastly, at high RH%, the SAXS shoulder peak intensity becomes lowest. The fact that the SAXS intensity decreased with increased relative humidity means the water molecules cannot be well-organized to form a larger water-rich amorphous domain rather gradually spread out homogeneously in the whole membrane. Our results from atomic force microscopy (AFM) observations also support the morphological change during hydration (see the Supporting Information).

Bragg spacings of crystallites including "rigid" amorphous domains with water were also investigated for every IEC. Bragg spacings were derived from the SAXS results of Figure 3b for the IEC:2.0 membrane and shown in Figure 5. It was found that the Bragg spacings hardly change with increasing relative humidity for every IEC sample. These results indicate that the volume of crystalline and amorphous domains does not change well even with increasing water in the membrane. We consider that rearrangement of polymer chains in the domain does not occur even though the volume of the crystalline domain decreases and the volume of the amorphous phase increases by sulfonation. Therefore, water might be uniformly distributed in the membrane with the increase of relative humidity.

No peak from the ionic domain was observed for sulfonated PPS membranes with varied IEC and different relative humidity. This suggests that, though small ionic aggregates exist in the membrane in the hydrated states, there is no scattering center of ionic−water cluster of a sufficiently high electron density to give rise to a peak. As described above, as the PPS chains are very rigid and do not have any pendant chain, the hydrophilic end groups cannot aggregate within a hydrophobic matrix, like the Nafion−water system.[34]

States of Polymer−Water Interface and Their Effects on Proton Conduction. The nature of water, i.e., the different states of water existing in the hydrophilic domains, is of great fundamental importance in understanding the influence of chemical structure on transport properties.[35] Three kinds of water

SCHEME 3: Three-Dimensional Schematic Diagram of States of Water Molecules in the SPPS Membrane under Hydrated Conditions

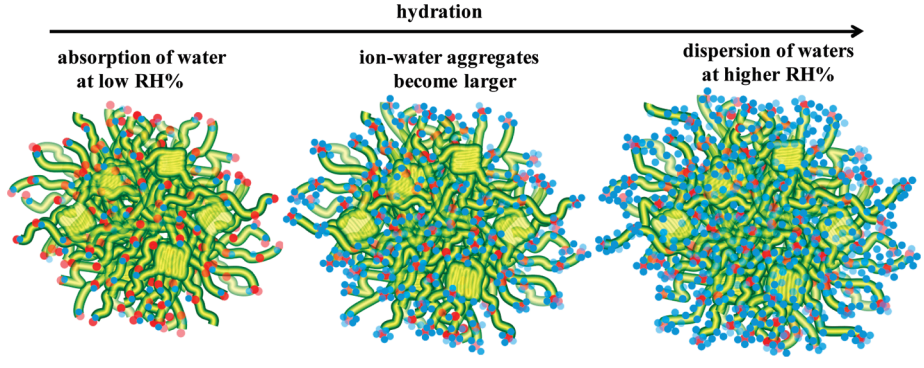

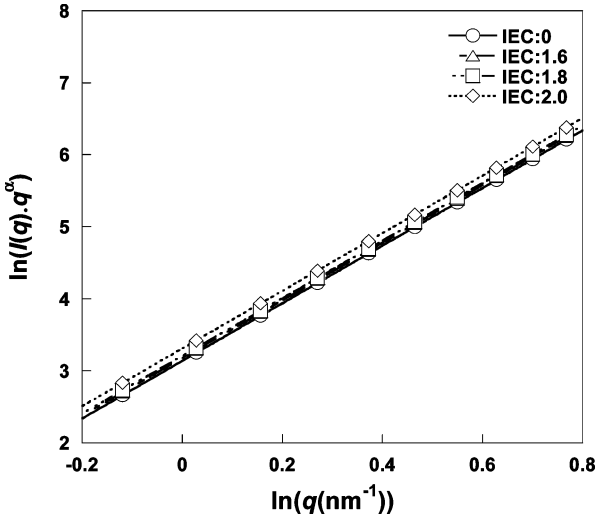

Figure 6. Porod fitting for SPPS membranes with varied IEC at 80% RH. The Porod plots showed "positive deviation".

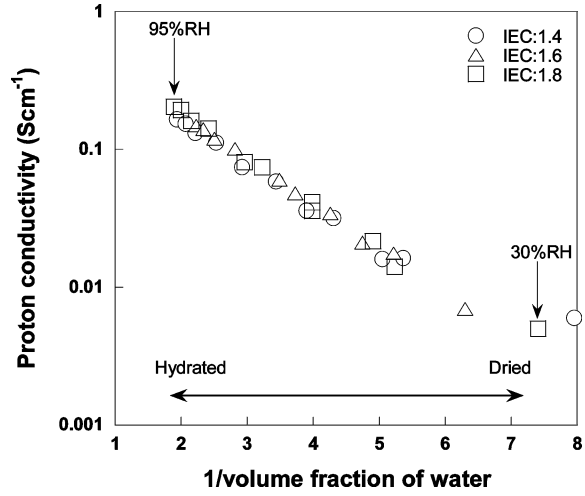

Figure 7. Proton conductivity for SPPS membranes with varied IEC as a function of the volume fraction of water at 80 °C.

exist in the sulfonated perfluoropolymer membrane: monomolecular water, clustered water, and structural water.[36] The state of the polymer/water interface is the key issue to develop proton channel formation in the sulfonated membranes. If the interface is not smooth but rather diffused, it becomes difficult to develop a proton channel to pass protons in the membrane. Also, if the ionic aggregates are distributed randomly and discontinued in the polymer matrix, protons cannot pass effectively through the interfacial region. Porod analysis from SAXS measurements is very efficient for extracting interface information and has been used for many years.[37,38] Porod fitting of the experimental SAXS profiles for SPPS membranes was performed to analyze the sharpness of the polymer/water interface which is related to proton conduction. According to the Porod law, for an obvious phase separated system, the intensity of scattering at large q follows the formula

$$\lim_{q\to\infty} q^4 I(q) = k_p \tag{6}$$

where k_p is the Porod constant and $I(q)$ is the scattering intensity.[39]

SAXS results were analyzed on the basis of the Porod law to deduce the interfacial structures in the humidified conditions, and the Porod plots for varied IEC at 80% RH are shown in Figure 6. The plots showed not a constant but "positive deviation", and this deviation from the Porod law indicates a diffuse interface in a two-phase system; i.e., in SPPS membrane, the polymer/water interface is not smooth but diffused in the hydrated conditions. The value of the slope (α) of the linear part of the Porod q-region was obtained as around -7.0, which for every IEC sample were almost identical and is much larger than the typical value of $\alpha = -4$ for an ideal two-phase system of sharp and smooth boundary.[40] The results also showed that the structural properties are not changed by the effect of the polymer/water interface in the hydrated conditions even though the IEC increases, which is consistent with the result of the proton conductivity measurement (Figure 7). In the case of Nafion, an increase of the amount of water molecules leads to larger ionic domains by rearrangement of polymer chains, but for SPPS, the size of ionic aggregates are comparatively smaller so large ionic domains cannot develop, rather smaller ionic aggregates remain randomly distributed. The reason for this may be that the ionic groups ($-SO_3H$) are only statistically attached to the rigid main chains of PPS during the sulfonation process and the rigid PPS backbones cannot bend to come closer to develop well-defined hydrophobic and hydrophilic phases. Due to the lack of flexibility, it becomes difficult for the ionic sequences to rearrange and develop ionic−water clusters even with an increase of water in the membrane.

In a previous paper, our group has demonstrated the difference in structural property of Nafion and HC-type ionomer membranes through the proton conductivity−water uptake relationship.[25] Figure 7 shows the effect of water uptake on proton conductivity for SPPS membranes measured at 80 °C. It was noted that proton conductivities for varied IEC is almost identical, which suggests that, although water uptake increases with IEC level, the effectiveness of proton conduction with water uptake does not change among the SPPS membranes. The results reveal that the morphological features such as ionic−water aggregation, aggregate connectivity, and width of the proton channels which pass protons through the membrane might be similar among the SPPS membranes.

4. Conclusions

An investigation on the effect of water on SPPS electrolyte membranes by various experimental techniques provided important insight regarding the changes of their morphological features. A systematic and fundamental study of SPPS membranes with varied IEC which was directly sulfonated from pristine PPS membrane was succeeded. At relatively lower humidity, the water affinity of $-SO_3H$ ionic groups is high, which makes smaller ion−water aggregates. The aggregates became larger at 50% RH, but at higher humidity, the water−water hydrogen bond interaction becomes stronger than the ion−water affinity. The water molecules cannot be well-organized to form a larger ionic cluster; rather, waters gradually spread out homogeneously in the whole membrane, which thus decreases the SAXS shoulder peak intensity. No SAXS peak from the ionic domain was observed for SPPS membranes with varied IEC and different relative humidity, which suggested that, though small ionic aggregates existed in the membranes, the ionic−water domain of a sufficiently high electron density was not formed to give rise to a peak. The Porod plot showed positive deviation which revealed that the polymer/water interface in the hydrated SPPS membranes of low to high IEC is not smooth but diffused. The rigidity of the PPS backbone

did not provide chain mobility for rearrangement of ionic−water aggregates to form a well-developed proton channel in hydrated SPPS membranes. Proton conductivities for varied IEC were almost identical, which suggested that the effectiveness of proton conduction with water uptake does not change among the SPPS membranes. Ionic−water aggregation, aggregation connectivity, and width of the proton channels for varied membranes might be similar among the SPPS membranes.

Acknowledgment. This work was financially supported by the Ministry of Economy, Trade and Industry (METI) and New Energy and Industrial Technology Development Organization (NEDO), Japan. We are grateful to KANEKA CORPORATION, Japan, for kindly providing the SPPS samples.

Supporting Information Available: Description of atomic force microscopy (AFM) observation for water humidified SPPS membranes and figures showing typical AFM phase images of SPPS membrane. This material is available free of charge via the Internet at http://pubs.acs.org.

References and Notes

(1) Kreuer, K. D. *J. Membr. Sci.* **2001**, *185*, 29.
(2) Rikukawa, M.; Sanui, K. *Prog. Polym. Sci.* **2000**, *25*, 1463.
(3) Hickner, M. A.; Ghassemi, H.; Kim, Y. S.; Einsla, B. R.; McGrath, J. E. *Chem. Rev.* **2004**, *104*, 4587.
(4) Ramya, K.; Dhathathreyan, K. S. *J. Appl. Polym. Sci.* **2003**, *88*, 307.
(5) Einsla, M. L.; Kim, Y. S.; Hawley, M.; Lee, H. S.; McGrath, J. E.; Liu, B.; Guiver, M. D.; Pivovar, B. S. *Chem. Mater.* **2008**, *20*, 5636.
(6) Roy, A.; Lee, H. S.; McGrath, J. E. *Polymer* **2008**, *49*, 5037.
(7) Carbone, A.; Pedicini, R.; Portale, G.; Longoc, A.; D'Ilario, L.; Passalacqua, E. *J. Power Sources* **2006**, *163*, 18.
(8) Jiang, R.; Kunz, H. R.; Fenton, J. M. *J. Power Sources* **2005**, *150*, 120.
(9) Jones, D. J.; Rozière, J. *J. Membr. Sci.* **2001**, *185*, 41.
(10) Miyatake, K.; Chikashige, Y.; Higuchi, E.; Watanabe, M. *J. Am. Chem. Soc.* **2007**, *129*, 3879.
(11) Dai, H.; Guan, R.; Li, C.; Liu, J. *Solid State Ionics* **2007**, *178*, 339.
(12) Miyatake, K.; Chikashige, Y.; Watanabe, M. *Macromolecules* **2003**, *36*, 9691.
(13) Kang, M. S.; Choi, Y. J.; Choi, I. J.; Yoon, T. H.; Moon, S. H. *J. Membr. Sci.* **2003**, *216*, 39.
(14) Nolte, R.; Ledjeff, K.; Bauer, M.; Mülhaupt, R. *J. Membr. Sci.* **1993**, *83*, 211.
(15) Wu, S.; Qiu, Z.; Zhang, S.; Yang, X.; Yang, F.; Li, Z. *Polymer* **2006**, *47*, 6993.
(16) Fujimoto, H.; Hickner, M. A.; Cornelius, C. J.; Loy, D. A. *Macromolecules* **2005**, *38*, 5010.
(17) Kobayashi, T.; Rikukawa, M.; Sanui, K.; Ogata, N. *Solid State Ionics* **1998**, *106*, 219.
(18) Kim, S.; Jackiw, J.; Robinson, E.; Schanze, K. S.; Reynolds, J. R.; Baur, J.; Rubner, M. F.; Boils, D. *Macromolecules* **1998**, *31*, 964.
(19) Vielstich, W.; Lamm, A.; Gasteiger, H. *Handbook of Fuel Cells: Fundamentals, Technology, and Applications*; Wiley: Hoboken, NJ, 2003.
(20) Cheng, S. Z. D.; Wu, Q.; Wunderlich, B. *Macromolecules* **1987**, *20*, 2802.
(21) Lu, D.; Mai, Y. W.; Li, R. K. Y.; Ye, L. *Macromol. Mater. Eng.* **2003**, *288*, 693.
(22) Schauer, J.; Kůdelaa, V.; Richaub, K.; Mohr, R. *Desalination* **2006**, *198*, 256.
(23) Schuster, M.; Araujo, C. d.; Atanasov, V.; Andersen, H. T.; Kreuer, K. D.; Maier, J. *Macromolecules* **2009**, *42*, 3129.
(24) Hidekazu, K.; Kiyoyuki, N. European Patent EP 1380 619A1, Jan 2004.
(25) Takimoto, N.; Wu, L.; Ohira, A.; Takeoka, Y.; Rikukawa, M. *Polymer* **2009**, *50*, 534.
(26) Napolitano, R.; Pirozzi, B.; Salvione, A. *Macromolecules* **1999**, *32*, 7682.
(27) Ballirano, P.; Caminiti, R.; D'ilario, L.; Martinelli, A.; Piozzi, A.; Maras, A. *J. Mater. Sci.* **1998**, *33*, 3519.
(28) Hay, J. N.; Luck, D. A. *Polymer* **2001**, *42*, 8297.
(29) Swier, S.; Chun, Y. S.; Gasa, J.; Shaw, M. T.; Weiss, R. A. *Polym. Eng. Sci.* **2005**, *45*, 1081.
(30) Guhathakurta, S.; Min, K. *Polymer* **2009**, *50*, 1034.
(31) Jin, X.; Bishop, M. T.; Ellis, T. S.; Karasz, F. E. *Br. Polym J* **1985**, *17*, 4.
(32) Chen, J. H.; Liu, Q. L.; Zhu, A. M.; Fang, J.; Zhang, Q. G. *J. Membr. Sci.* **2008**, *308*, 171.
(33) Lu, S. X.; Capel, Cebe, P. *Macromolecules* **1997**, *30*, 6243.
(34) Mauritz, K. A.; Moore, R. B. *Chem. Rev.* **2004**, *104*, 4535.
(35) Kim, Y. S.; Dong, L.; Hickner, M. A.; Glass, T. E.; Webb, V.; McGrath, J. E. *Macromolecules* **2003**, *36*, 6281.
(36) Takata, H.; Mizuno, N.; Nishikawa, M.; Fukada, S.; Yoshitake, M. *Int. J. Hydrogen Energy* **2007**, *32*, 371.
(37) Ruland, W. *Macromolecules* **1987**, *20*, 87.
(38) Jung, W. G.; Fischer, E. W. *Makromol. Chem. Makromol. Symp.* **1988**, *16*, 281.
(39) Zhao, C.; Li, X.; Wang, Z.; Dou, Z.; Zhong, S.; Na, H. *J. Membr. Sci.* **2006**, *280*, 643.
(40) Sen, D.; Bahadur, J.; Mazumder, S.; Bedekar, V.; Tyagi, A. K. *J. Phys.: Condens. Matter* **2008**, *20*, 035103.

JP905297M